

# POLYGON FEATURE EXTRACTION FROM SATELLITE IMAGERY BASED ON COLOUR IMAGE SEGMENTATION AND MEDIAL AXIS

Ojaswa Sharma<sup>†</sup>, Darka Mioc<sup>‡</sup> and François Anton<sup>†</sup>

<sup>†</sup> Image Analysis and Computer Graphics,  
DTU Informatics, Technical University of Denmark,  
Richard Petersens Plads, bldg. 321,  
DK-2800 Kgs. Lyngby, Denmark  
{os, fa}@imm.dtu.dk

<sup>‡</sup> Dept. of Geodesy and Geomatics Engineering,  
University of New Brunswick, P.O. Box 4400,  
Fredericton NB Canada E3B 5A3,  
dmioc@unb.ca

Commission III/3

**KEY WORDS:** Feature, Extraction, Imagery, Segmentation, Semi-automation

## ABSTRACT:

Areal features are of great importance in applications like shore line mapping, boundary delineation and change detection. This research work is an attempt to automate the process of extracting feature boundaries from satellite imagery. This process is intended to eventually replace manual digitization by computer assisted boundary detection and conversion to a vector layer in a Geographic Information System. Another potential application is to be able to use the extracted linear features in image matching algorithms. In multi-spectral satellite imagery, various features can be distinguished based on their colour. There has been a good amount of work already done as far as boundary detection and skeletonization is concerned, but this research work is different from the previous ones in the way that it uses the Delaunay graph and the Voronoi tessellation to extract boundary and skeletons that are guaranteed to be topologically equivalent to the segmented objects. The features thus extracted as object border can be stored as vector maps in a Geographic Information System after labelling and editing. Here we present a complete methodology of the skeletonization process from satellite imagery using a colour image segmentation algorithm with examples of road networks and hydrographic networks.

## 1 INTRODUCTION

With the advent of multi-spectral and high resolution satellite imagery, we have more information that can be processed to generate better representations of the features of the earth. Classical edge detection algorithms or segmentation methods do not take full advantage of the color information that these images contain. A comparatively new and efficient segmentation algorithm by Comaniciu and Meer (Comaniciu and Meer, 2002) uses feature space analysis to segment multi-spectral images. Prominent features are located using the mean shift algorithm in the feature space of the image. This algorithm detects significant colors from the image. Thus, it is possible to suppress minor variations in the hue of objects present in the image. The mean shift algorithm works very well on color images and is able to resolve features to a great extent. A modification of the algorithm can also tolerate intensity variations within the same hue.

Feature extraction from satellite images has been studied by many researchers. A technique for coastline extraction from remotely sensed images using texture analysis is described in (Bo et al., 2001). The delineation of the complete coastline of Antarctica using SAR imagery is shown in (Liu and Jezek, 2004). A morphological segmentation based automated approach for coastline extraction has been suggested in (Bagli and Soille, 2003). Di et al. use the image segmentation algorithm by Comaniciu and Meer (Comaniciu and Meer, 2002) to segment an image and detect the shoreline (Di et al., 2003). Our work in progress is an extension to the work by Gold and Snoeyink (Gold and Snoeyink, 2001). Our boundary (crust) extraction algorithm converts detected image features into connected sets of vectors that are topologically

equivalent to the segmented objects. We claim topological equivalence of the extracted features since these are obtained as subsets of the Voronoi diagram or the Delaunay triangulation.

## 2 IMAGE SEGMENTATION

Edge detection produces global edges in an image. This means that there is no object definition attached to the edges. Therefore it is required to somehow define the objects first and then obtain edges from them. This can be achieved by using *image segmentation*. The main goal of image segmentation is to divide an image into parts that have a strong correlation with objects or areas of the real world depicted in the image (Sonka et al., 1999, chap. 5). Thus, image segmentation divides the whole image into homogeneous regions based on colour information. The regions can be loosely defined as representatives of objects present in the image.

Feature space analysis is used extensively in image understanding tasks. Comaniciu and Meer (Comaniciu and Meer, 1997) provide a comparatively new and efficient segmentation algorithm that is based on feature space analysis and relies on the *mean-shift algorithm* to robustly determine the cluster means. A *feature space* is a space of feature vectors. These features can be object descriptors or patterns in case of an image. As an example, if we consider a colour image having three bands (red, green, and blue) then the image we see as intensity values plotted in Euclidean XY space is said to be in *image space*. Consider a three dimensional space with the axes being the three bands of the image. Each colour vector corresponding to a pixel from the image can be represented as point in the feature space.

Given  $n$  data points  $x_i, i = 1, \dots, n$  in the  $d$ -dimensional space  $R^d$ , a flat kernel that is characteristic function of the  $\lambda$ -ball in  $R^d$  is defined as

$$K(x) = \begin{cases} 1 & \text{if } \|x\| \leq \lambda \\ 0 & \text{if } \|x\| > \lambda \end{cases} \quad (1)$$

The mean shift vector at a location  $x$  is defined as

$$M_\lambda(x) = \frac{\sum_{r \in R^d} K(r-x)r}{\sum_{r \in R^d} K(r-x)} - x \quad (2)$$

Cheng (Cheng, 1995) shows that the mean shift vector, the vector of difference between the local mean and the center of the window  $K(x)$ , is proportional to the gradient of the probability density at  $x$ . Thus mean shift is the steepest ascent with a varying step size that is the magnitude of the gradient. Comaniciu and Meer (Comaniciu and Meer, 2002) use mean shift vector in seeking the mode of a density by shifting the kernel window by the magnitude of the mean shift vector repeatedly. The authors also prove that the mean shift vector converges to zero and eventually reaches the basin of attraction of that mode.

Comaniciu and Meer (Comaniciu and Meer, 1997) state a simple, adaptive steepest ascent mode seeking (Cheng, 1995) algorithm.

1. Choose the radius  $r$  of the search window (i.e, radius of the kernel).
2. Choose the initial location of the window.
3. Compute the mean shift vector and translate the search window by that amount.
4. Repeat until convergence.

An application of the mean shift algorithm based colour image segmentation is illustrated in Figure 1. The Mean shift algorithm gives a general technique of clustering multi-dimensional data and is applied here in colour image segmentation. The fundamental use of mean shift is in seeking the modes that gives that regions of high density in any data.

Later, Comaniciu and Meer provide an improvement (Comaniciu and Meer, 2002) over this segmentation algorithm by merging the image domain and the feature (range) space into a joint spatial-range domain of dimension  $d = p + 2$ , where  $p$  is the dimension of the range domain. This gives an added advantage of considering both the spaces together and gives good results in cases where non-uniform illumination produces false contours when the previous segmentation algorithm is used. Therefore, the new algorithm is particularly useful to segment natural images with man-made objects. An added computational overhead to process higher dimensional space is inevitable here.

Segmentation provides us with definite object boundary by means of simple edge detection. We use morphological edge detection on a user selected binary region, which is a combination of one or more segments. All the edge pixels are then considered as sample points around objects of interest. These sample points can be used then to compute the skeleton and the boundary of the object as discussed next.



(a) Original image (b) Segmented image

Figure 1: Result of colour image segmentation on a natural image.

### 3 CRUST EXTRACTION FROM THE DELAUNAY TRIANGULATION

The vertices of the Voronoi diagram approximate the medial axis of a set points sampled along the boundary of an object. In their research, vertices of the Voronoi diagram of the sample points were inserted into the original set of sample points and a new Delaunay triangulation was computed. The circumcircles of this new triangulation approximate empty circles between the original boundary of the object and its skeleton. Thus, they conclude that any Delaunay edge connecting a pair of the original sample points in the new triangulation is a part of the border.

Further, paper by Gold (Gold, 1999) leads to a One-step border (crust) extraction algorithm. In a Delaunay triangulation, each Delaunay edge is adjacent to two triangles and the circumcircles of these triangles are the Voronoi vertices. A Voronoi edge connecting these two circumcenters is the dual edge to the Delaunay edge considered here. According to Gold (Gold, 1999), a Delaunay edge is a part of the border if it has a circle passing through its extremities that does not contain any Voronoi vertex in its interior. The test is the standard *InCircle* test. Considering two triangles  $(p, q, r)$  and  $(r, q, s)$  sharing an edge  $(q, r)$  in a Delaunay triangulation and let  $v$  be the a vector orthogonal to edge  $(r - q)$  in clockwise order, then the test becomes:

$$(s - q) \cdot (s - r) * (p - q) \cdot (p - r) \geq - (s - r) \cdot v * (p - q) \cdot v \quad (3)$$

This test will be true for an edge in the border set. Furthermore, those Delaunay edges that do not belong to the border set have their dual Voronoi edges in the skeleton (shown in Figure 2).

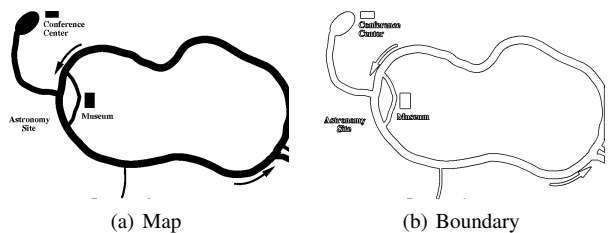


Figure 2: Result of boundary (crust) extraction using algorithm by Gold.

### 4 MEDIAL AXIS EXTRACTION FROM DETECTED FEATURE

The work of Amenta (Amenta et al., 1998) shows that the “crust” or the boundary of a polygon can be extracted from an unstructured set of points, provided the data points are well sampled. Gold and Snoeyink (Gold and Snoeyink, 2001) further simplify their method and show that the boundary can be extracted in a single step (see section 3). Gold (Gold, 1999) discusses about

“anti-crust” in context of skeleton extraction citing a brief introduction of this term in (Amenta et al., 1998). The idea behind getting skeleton is that a Voronoi edge is a part of the skeleton if its corresponding dual Delaunay edge is not a part of the border set (crust) and it lies completely within the selected object. Thus, selecting the Voronoi edges lying inside the selected object that are dual of the non-crust Delaunay edges should give us the skeleton (see Figure 3). The Voronoi edges thus selected form a tree structure called the “anti-crust” (Gold, 1999) that extend towards the boundary but do not cross it.

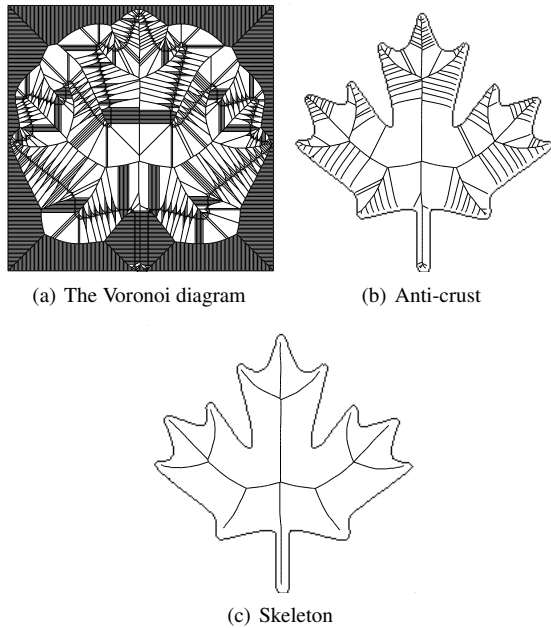


Figure 3: Skeleton as seen as the anti-crust.

Research by NN (Anton et al., 2001) suggests a new algorithm for skeleton extraction. This is based on the concept of *Gabriel Graph* (Gabriel and Sokal, 1969). A Gabriel graph  $G$  (highlighted in Figure 5) is a connected subset of the Delaunay graph  $\mathcal{D}$  of points in set  $S$  such that two points  $p_i$  and  $p_j$  in  $S$  are connected by an edge of the Gabriel graph, if and only if, the circle with diameter  $p_i p_j$  does not contain any other point of  $S$  in its interior. In other words, the edges in  $G$  are those edges from  $\mathcal{D}$  whose dual Voronoi edges intersect with them. Consider four points  $p_i, p_j, p_k$ , and  $p_l$  on a plane. Figure 4(a) shows Gabriel edge  $p_i p_j$  that satisfies the empty circle criterion. Circles  $C'$  and  $C''$  are circumcircles of triangles  $p_j p_i p_k$  and  $p_i p_j p_l$  respectively and circle  $C$  is a circle with diameter as edge  $p_i p_j$ . Figure 4(b) shows the case when the Gabriel condition is not met.

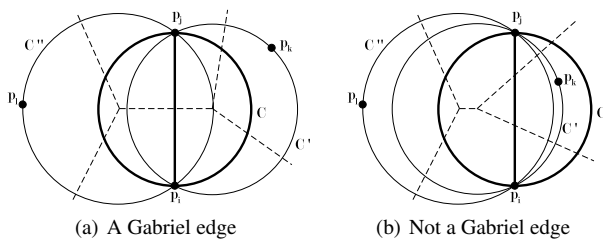


Figure 4: Condition for Gabriel edge.

Given the Delaunay triangulation  $\mathcal{D}$  and the Voronoi diagram  $V$  of sample points  $S$  from the boundary of an object, the algorithm for centreline extraction in (Anton et al., 2001) proceeds by selecting all the Gabriel edges in graph  $G$ . Each dual Voronoi edge  $v$

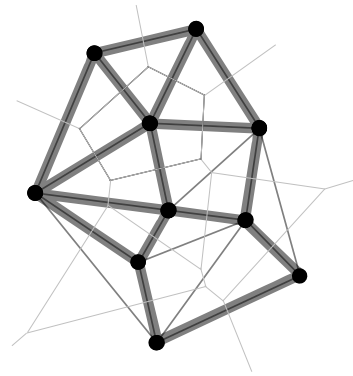


Figure 5: Gabriel graph highlighted in a Delaunay triangulation.

of the Gabriel edge  $g$  from  $G$  is inserted in the skeleton  $K$  if the following condition is met:

$$\begin{aligned}
 &g.Origin.Colour \neq g.Destination.Colour \\
 &\quad \text{Or} \\
 &g.Origin.Colour \neq v.Origin.Colour \\
 &\quad \text{Or} \\
 &g.Origin.Colour \neq v.Destination.Colour \quad (4) \\
 &\quad \text{And} \\
 &\|g.Origin.Colour - g.Dest.Colour\| \geq \\
 &\|v.Origin.Colour - v.Dest.Colour\|
 \end{aligned}$$

Here, *Origin.Colour* and *Destination.Colour* are colour values (digital number) from the gray scale image corresponding to the location of the origin and the destination of an edge respectively. Figure 6(b) shows the result of skeleton extraction from streams present in a map (Figure 6(a)). However, a close observation reveals that the skeleton thus obtained has gaps. These gaps are prominent if the object under consideration has sharp turns in its geometry which is further amplified if the object is thick. We have found a way to overcome this by locating skeleton edges by moving along the border set. Current research in progress tries to overcome this, but we do not use this approach in this paper.

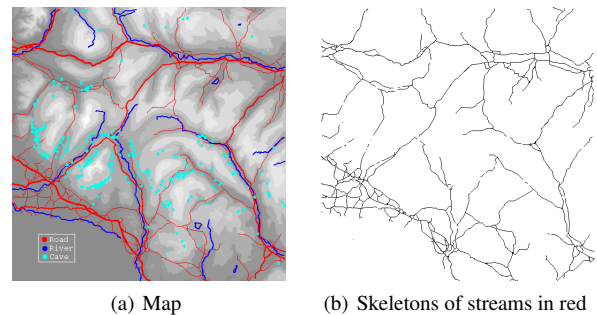


Figure 6: Result of skeleton extraction using the algorithm by (NN for anonymity).

#### 4.1 Obtaining Anti-crust from the Voronoi diagram

The anti-crust of an object, as described above, forms a tree like structure that contains the skeleton. Once all the Delaunay edges belonging to the border set or the crust are identified using the condition given by Gold (Gold, 1999), it is easy to identify the Voronoi edges belonging to the anti-crust. In Figure 7, consider the Delaunay triangulation (dashed edges), the corresponding Voronoi diagram (dotted edges) and the crust edges (solid red edges).

Navigation from a Delaunay edge to its dual Voronoi edge can be achieved by using the *Rot()* operator in the quad-edge data

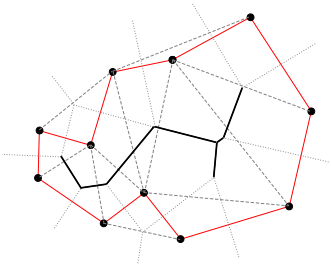


Figure 7: Anti-crust from the crust.

structure (Guibas and Stolfi, 1985). A Voronoi edge  $e.Rot()$  of the dual Delaunay edge  $e$  is marked as an edge belonging to the anti-crust if the following conditions are satisfied:

1.  $e \notin Crust$
2.  $e.Rot().Origin \in I$
3.  $e.Rot().Destination \in I$

where  $e.Rot().Origin$  is the origin of the edge  $e.Rot()$ ,  $e.Rot().Destination$  is the destination of the edge  $e.Rot()$  and  $I$  is the selected object. This marks all the Voronoi edges belonging to the anti-crust that fall inside the selected object. Negating conditions (2) and (3) so that the points do not fall inside the object will give us the exterior skeleton or the *exoskeleton*. Once the anti-crust is identified, an appropriate pruning method can be applied to get rid of the unwanted edges.

#### 4.2 Pruning

Gold (Gold, 1999) also discusses about the “hairs” around the skeleton that result due to the presence of three adjacent sample points whose circumcircle does not contain any other sample point - either near the end of a main skeleton branch or at locations on the boundary where there is minor perturbation because of raster sampling. Gold and Thibault (Gold and Thibault, 2001) suggest a skeleton retraction scheme in order to get rid of the hairs that also results in smoothing of the boundary of the object. Ogniewicz (Ogniewicz, 1994) presents an elaborate skeleton pruning scheme based on various residual functions. Thus, a hierarchic skeleton is created which is good for multiscale representation. NN (Sharma et al., 2005) suggest the use of ratio based pruning in order to simplify a network of skeletons for extracting linear features from satellite imagery.

The problem of identifying skeleton edges now reduces to reasonably prune the anti-crust. We next present an optimal criterion for pruning by successively removing leaf edges from the anti-crust.

#### 4.3 Pruning by Removing Leaf Edges

Gold and Thibault (Gold and Thibault, 2001) present a retraction scheme for the leaf nodes in the anti-crust. The skeleton is simplified by retracting the leaf nodes of the skeleton to their parent nodes. Gold and Thibault (Gold and Thibault, 2001) recommend performing the retraction operation repeatedly until no further changes take place. An observation reveals that an unwanted branch in a skeleton may be composed of more than one edge (see Figure 8). Therefore, single retraction may not be sufficient to provide an acceptable skeleton.

A similar simplification can be achieved by pruning the leaf edges instead of retracting the leaf nodes. Leaf edge pruning produces

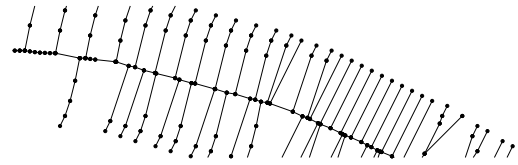


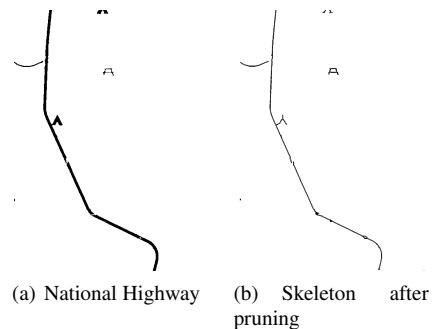
Figure 8: Hair around the skeleton composed of multiple edges.

satisfactory results and requires only two or three levels of pruning. Before pruning the leaf edges, they must be identified in the anti-crust. An edge  $e$  from a tree of edges  $T \in V$ , where  $V$  is the Voronoi diagram, is marked as a leaf edge if the following condition is satisfied

$$\begin{aligned}
 &e.Opnev() \notin T \text{ And } e.Onext() \notin T \\
 &\text{Or} \\
 &e.Sym().Opnev() \notin T \text{ And } e.Sym().Onext() \notin T
 \end{aligned} \tag{5}$$

This condition essentially selects all the Voronoi edges belonging to the anti-crust that have at least one end point free (i.e., connected to an edge not belonging to the anti-crust). This condition is used to locate leaf edges followed by their removal from the skeleton. Experiments show that removing leaf edges two to three times simplifies the skeleton to a major extent for linear features.

We find an optimal criterion for removal of extraneous hair from the skeleton by pruning the leaf edges. Figure 9(a) shows a thick linear feature. Such linear features appear in the form of boundaries of some features like roads. The result of leaf edge pruning is shown in Figure 9(b). A plot of the edges pruned in every iteration (see Figure 9(c)) underlines the fact that first two iterations are enough to produce an acceptable skeleton and that further pruning results in mere contraction of the skeleton (indicated by the horizontal plot after a steep drop after third iteration).



(a) National Highway (b) Skeleton after pruning



(c) Pruning plot of object

Figure 9: Skeleton obtained after pruning leaf edges.

## 5 RESULTS

The following examples show extraction of the boundary of the selected object. The accuracy of the boundary rendition depends on the spatial resolution of the imagery. A few cases of road network and hydrography network have been considered here. Figure 10 shows the complex coastline of Guinea Bissau. Segmentation results in four colours that define the water body out of which three define the coastline. Multiple selection enables combining these three regions together to form the complete coastline as shown in Figure 10(d).

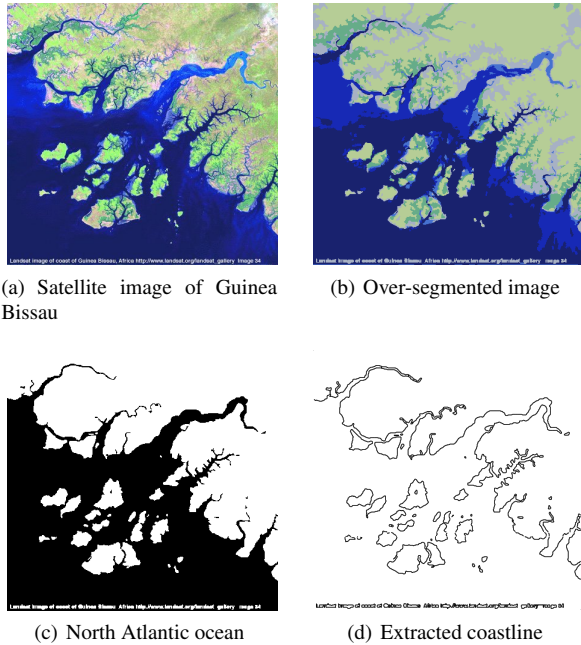


Figure 10: Feature polygon extraction from the satellite image of Guinea Bissau.

A satellite image of Lake Jempang, East Kalimantan, Indonesia (20 Jul 2002) obtained online from Centre for Remote Imaging, Sensing and Processing ([http://www.crisp.nus.edu.sg/monthly\\_scenes/y2002/Jul02\\_i.html](http://www.crisp.nus.edu.sg/monthly_scenes/y2002/Jul02_i.html)) is shown in Figure 11(a). The extracted lake boundary is shown in Figure 11(d).

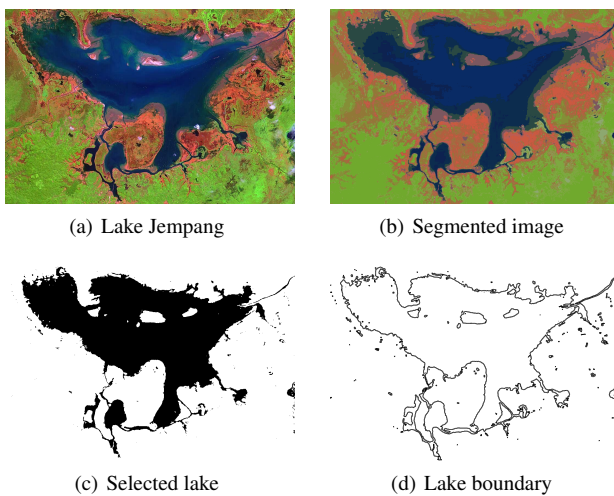


Figure 11: SPOT satellite image of Lake Jempang, East Kalimantan, Indonesia (20 Jul 2002).

We show extraction of road in Figure 12, where the trans-canadian highway and the adjoining road network has been extracted. The extracted highway and associated the road network is shown in Figure 12(d).

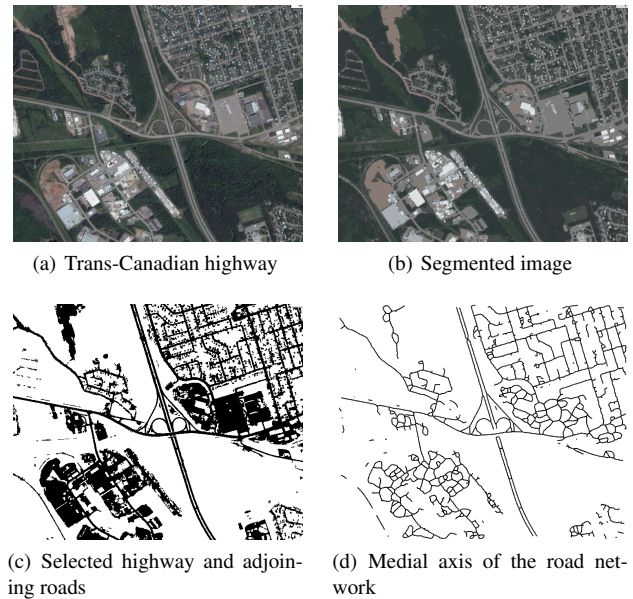


Figure 12: Satellite image of the trans-Canadian Highway, Moncton, Canada.

Another case of road network is shown in Figure 13. The roads delineating the fields are extracted (shown in Figure 13(b)).

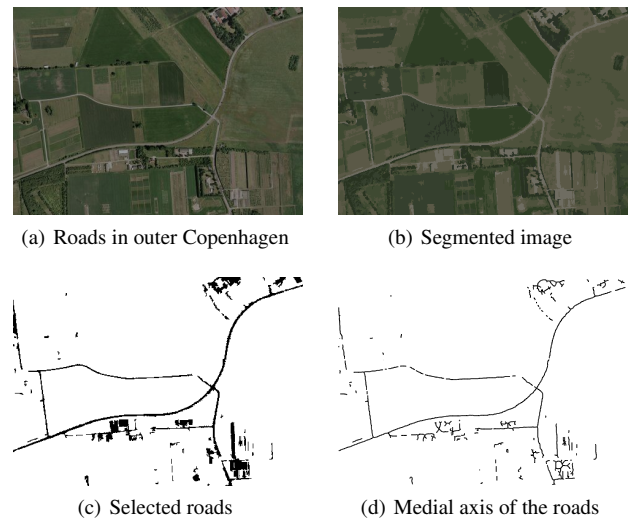


Figure 13: Roads in outer Copenhagen, Denmark.

## 6 TIME COMPLEXITY

It is important to analyse the complete procedure for time complexity. Since the overall complexity will depend on the intermediate steps, these are first analysed individually.

Comaniciu (Comaniciu, 2000, p. 21) shows that the complexity of the probabilistic mean shift type algorithm that is employed in the segmentation algorithm (Comaniciu and Meer, 1997) is  $O(mn)$ , with  $m \ll n$  where  $n$  is the number of pixels in the input

image (or the number of feature vectors in the feature space) and  $m$  is the number of vectors in initial feature palette or clusters. Comaniciu (Comaniciu, 2000, p. 29) claims that the segmentation algorithm is linear with the number of pixels in the image.

Object selection is implemented as a simple search of pixel colour values compared with the user selected points on the image. Therefore, it is  $O(n)$  with the number of pixels  $n$  in the image.

Binary edge detection is implemented as subtraction of two binary images. One of the binary images is always the original image while the other is either a dilated or an eroded image of the original. For an image  $I$  of size  $x \times y$  and a structural element of size  $k \times l$ , computation of either erosion or dilation requires  $x \times y$  iterations, each requiring  $(k \times l) + 1$  comparisons. Therefore, the time complexity is linear with number of pixels of the input binary image and linear with the area of the structural element. Overall time complexity can be said to be  $O(mn)$  where  $n$  is number of pixels in the image and  $m$  is number of pixels in the structuring element. Further, in the structural element, only locations having a value of 1 are considered in the computations. In our case, the application uses a  $3 \times 3$  structural element with only five values being 1's in the mask (i.e.,  $m = 5$ ). Therefore, we can safely say that edge detection is  $O(n)$  with the number of pixels  $n$  in the image.

## 7 CONCLUSIONS

Our results show a promising machinery to extract meaningful features from remote sensing image data. Coastlines, dense forests, fields and roads are among a few features that can be extracted in a semi-automated manner. The added advantage of our method is that the results are not just a series of connected pixels or sets of line segments, rather they offer spatial information and connectivity for free. A prototype application has been developed as part of the research to show a practical application of the approach. The application integrates the techniques explored and developed during the research. It allows to read colour images and perform segmentation on them. Identified features can be sampled for boundary that is used to compute the Voronoi and Delaunay graph. The boundary and skeleton extraction algorithm then extracts the required features.

A few other applications, where satisfactory results can be obtained, include snow cover mapping, cloud detection, and dense forest mapping.

## 8 LIMITATIONS

The segmentation algorithm (Comaniciu and Meer, 1997) may result in misclassification depending on the image quality and the parameters chosen for segmentation. Some image pre-processing is suggested for such cases.

## REFERENCES

- Amenta, N., Bern, M. and Eppstein, D., 1998. The crust and the  $\beta$ -skeleton: Combinatorial curve reconstruction. *Graphical models and image processing: GMIP 60(2)*, pp. 125–135.
- Anton, F., Mioc, D. and Fournier, A., 2001. 2D image reconstruction using natural neighbour interpolation. *The Visual Computer* 17(3), pp. 134–146.
- Bagli, S. and Soille, P., 2003. Morphological automatic extraction of coastline from pan-european landsat tm images. In: *Proceedings of the Fifth International Symposium on GIS and Computer Cartography for Coastal Zone Management*, Vol. 3, Genova, pp. 58–59.
- Bo, G., Delleplane, S. and Laurentiis, R. D., 2001. Coastline extraction in remotely sensed images by means of texture features analysis. In: *Geoscience and Remote Sensing Symposium, IGARSS '01*, Vol. 3, Sydney, NSW, Australia, pp. 1493–1495.
- Cheng, Y., 1995. Mean shift, mode seeking, and clustering. *IEEE Transactions on Pattern Analysis and Machine Intelligence* 17(8), pp. 790–799.
- Comaniciu, D. and Meer, P., 1997. Robust analysis of feature spaces: color image segmentation. In: *Proceedings of the 1997 Conference on Computer Vision and Pattern Recognition (CVPR '97)*, IEEE Computer Society, Washington, DC, USA, pp. 750–755.
- Comaniciu, D. and Meer, P., 2002. Mean shift: A robust approach toward feature space analysis. *IEEE Transactions on Pattern Analysis Machine Intelligence* 24(5), pp. 603–619.
- Comaniciu, D. I., 2000. *Non-Parametric Robust Methods for Computer Vision*. PhD thesis, Rutgers, The State University of New Jersey.
- Di, K., Wang, J., Ma, R. and Li, R., 2003. Automatic shoreline extraction from high-resolution ikonos satellite imagery. In: *Proceeding of ASPRS 2003 Annual Conference*, Vol. 3, Anchorage, Alaska.
- Gabriel, K. R. and Sokal, R. R., 1969. A new statistical approach to geographic variation analysis. *Systematic Zoology* 18(3), pp. 259–278.
- Gold, C. M., 1999. Crust and anti-crust: A one-step boundary and skeleton extraction algorithm. In: *Symposium on Computational Geometry*, ACM Press, New York, NY, USA, pp. 189–196.
- Gold, C. M. and Snoeyink, J., 2001. A one-step crust and skeleton extraction algorithm. *Algorithmica* 30(2), pp. 144–163.
- Gold, C. M. and Thibault, D., 2001. Map generalization by skeleton retraction. In: *Proceedings of the 20th International Cartographic Conference (ICC)*, Beijing, China, pp. 2072–2081.
- Guibas, L. and Stolfi, J., 1985. Primitives for the manipulation of general subdivisions and the computation of voronoi diagrams. *ACM Transactions on Graphics* 4(2), pp. 74–123.
- Liu, H. and Jezek, K. C., 2004. A complete high-resolution coastline of antarctica extracted from orthorectified radarsat sar imagery. *Photogrammetric Engineering and Remote Sensing* 70(5), pp. 605–616.
- Ogniewicz, R. L., 1994. Skeleton-space: A multiscale shape description combining region and boundary information. In: *Proceedings of Computer Vision and Pattern Recognition*, 1994, pp. 746–751.
- Sharma, O., Mioc, M. and Habib, A., 2005. Road extraction from satellite imagery using fractals and morphological image processing. In: *Proceedings of the 13th International Conference on Geoinformatics*, Toronto, Canada.
- Sonka, M., Hlavac, V. and Boyle, R., 1999. *Image Processing, Analysis, and Machine Vision*. PWS publishing.